Synthesis of Saturated and Unsaturated Curtis-Type Ni Derivatives as 2,6-Dihydroxyanthraquinonates. Crystal and Molecular Structure. Thin Film Measurements of Conductivity and ab Initio Calculations of Electronic States

J. Gómez-Lara,[†,‡] B. González-Rolón,[§] J. A. Cogordan,*[,‡] A. Ortíz,[||] G. Espinosa-Pérez,[‡] and S. Ríos[‡]

Instituto de Química and Instituto de Investigaciones en Materiales, Univerisad Nacional Autonoma de México, Circuito Exterior, C. U., 04510 Coyoacán, D.F. México, and Facultad de Ingeniería Mecánica y Eléctrica, Universidad de Guanajuato, Salamanca, Gto., México

Received March 8, 1999. Revised Manuscript Received April 18, 2000

Synthesis of two charge-transfer donor−acceptor systems, based on Curtis-type complexes, one saturated and the other unsaturated, as salts of anthraflavic acid (2,6-dihydroxyanthraquinone) and their chemical, crystal, and molecular characterization are reported as well as their conductivity in thin-film form when deposited by vacuum thermal evaporation. The absorption edge for the films was determined from the optical transmission spectra in the visible by applying the Tauc model. Ab initio calculations were carried out, and with the obtained electronic structure, local densities of states were computed.

Introduction

Metallomacrocyclic coordination derivatives have been the subject of studies related to different areas because of their potential application in material science,[1] nonlinear optics,[2] liquid crystals,[3] and Langmuir−Blodgett (LB) films.[4] Recently, pentaazamacrocyclic derivatives of Lu have been used as sequence-specific photocleavage of DNA.[5] Tetraaza macrocycles have suitable structural characteristics to prepare low-dimensional organic compounds. Curtis Ni complexes are of interest in this approach as one can change from nonsaturated to saturated systems or one can have several steroisomeric structures,[6] and they have an almost planar structure around the Ni ion. On the other hand, anthraquinone and its derivatives have large electronically delocalized systems which can easily be polarized. Therefore, partial charge transfer can be established.

We substituted the perchlorate anion, present as counterion in saturated and unsaturated Curtis macrocycles, with 2,6-hydroxyanthraquinone and determined the crystalline structures for the nonsaturated macrocycle and the corresponding saturated system as large ionic salts, which nevertheless have properties related to molecular solids. Recently, conductive organic molecular compounds have been the subject of extensive studies. A lot of this work has been carried out in polycrystalline samples.[7] Organic molecular solids are formed by condensation and organization of molecular units. Compounds reported here are similar in nature to these organic molecular solids due to the large size and chemical nature of the individual ions. Generally, these materials are formed by large molecules, 10 to 20 atoms and upward, which have intermolecular bonds of van der Waals type, although the atomic intramolecular bonds are of covalent nature.[8] There are several structural parameters that determine the condensed phase, besides the nature and magnitude of the intermolecular interaction, the resulting order and the symmetry of the crystalline packing are the most important. Often, the crystalline structure of these materials is formed by parallel linear chains, along which a high electrical conduction is observed.[9] These condensed materials can be classified as low-dimensional solids, due to their anisotropic properties.

As it is observed in amorphous inorganic semiconductors, loss of periodicity and subsequently their crystalline structure results in the localization of electronic wave functions with a turn of a tail in the function of density of states. In the edges of valence and conduction,

[†] In memoriam.
[‡] Instituto de Química.
[§] Universidad de Guanajuato.
[||] Instituto de Investigaciones en Materiales.

(1) Hanack M.; Lang M. *Adv. Mater.* **1994**, *6*, 819.
(2) Casstevens, M.; Samok, M.; Pfleger, J.; Prasad, P. N. *J. Chem. Phys.* **1990**, *92*, 2019.
(3) Van der Pol, J. F.; Neeleman E.; Zwikker, J. W.; Nolte, R. J. M.; Drenth, W.; Aerts, J.; Visser, R.; Picken, S. *J. Liq. Cryst.* **1989**, *6*, 577.
(4) Burghard, M.; Schmelzer M.; Roth, S.; Haishc, P.; Hanack M. *Langmuir* **1994**, *10*, 4265.
(5) Darren, M.; Wright, M.; Miller, R. A.; Sessler, J. L.; Sansom, P. I. *J. Am. Chem. Soc.* **1995**, *117*, 3629−3630.
(6) Wagner, L. G.; Busch, D. H. *J. Am. Chem. Soc.* **1969**, *91*, 4092−4101.
(7) Silinsh, E. A.; Capek, V. *Organic Molecular Crystals*; American Institute of Physics Press: New York, 1994.
(8) Kitaigorodsky, A. Y. *Molecular Crystals and Molecules*; Academic Press: New York, 1973.
(9) Williams, J. M.; Adv. *Inorg. Chem. Radiochem.* **1983**, *26*, 235. Rogers, M. L.; Martin, D. S. *Polyhedron* **1987**, *6*, 225.

10.1021/cm990138k CCC: $19.00
Published on Web 12/01/2000

bands extend into the forbidden gap. As a result, electrical conduction is explained by the hopping and tunneling mechanisms of charge transport, establishing a mobility edge for the charge carriers.[10]

Given the electrical properties presented by these materials, their application in the preparation of high-quality optoelectronic structures has a lot of potential; although at present, the electrical conduction mechanism is not well understood.[11] Recently, deposition of thin films of these materials by thermal evaporation has produced thin-film transistors and electroluminescent devices.[12,13]

Experimental Section

General Information. Elemental analyses were performed by Galbraith Laboratories. (*meso*-5,7,7,12,14,14-hexamethyl-1,4,8,11-tetraazacyclotetradeca-4,11-diene)Nickel (II) perchlorate and (*rac*-5,7,7,12,14,14-hexamethyl-1,4,8,11-tetraazacyclotetradecane)Nickel (II) perchlorate were prepared according to reported procedures.[14] Anthraflavic acid (2,6-dihydroxyanthraquinone) (Aldrich) was recrystallized from acetic acid. Routine infrared spectra were recorded on a Nicolet-Magna-IR 750 spectrophotometer as KBr pellets, and infrared spectra for the deposited thin films were measured with a FTIR spectrophotometer Nicolet 5X with an uncertainty of 4 cm^{-1}. X-ray spectra of the deposited films were obtained by means of a Siemens D-500 system. The ellipsometric measurements were made using a Gaertner L117 ellipsometer with a wavelength of 630 nm from a He−Ne laser. The current−voltage characteristics and the dependence of the electrical conductivity of the sample as a function of temperature in the range 123−473 K were measured with a Keithley 230 programmable voltage source and a Keithley 485 autoranging picoammeter, both PC-controlled. The temperature of the sample was measured with a chromel−alumel thermocouple attached to a HP 3421A data acquisition unit.

Synthesis of (*meso*-5,7,7,12,14,14-hexamethyl-1,4,8,11-tetraazacyclo-tetradeca-4,11-diene)Nickel(II) 2,6-dihydroxyanthraquinonate(I). Ni(*meso*-5,7,7−12,14,14-hexamethyl-1,4,8,11-tetraazacyclotetradeca-4,11-diene) perchlorate (0.7 g, 1.3×10^{-3} mol) dissolved in 50 mL of 1:1 (vol/vol) H_2O−ethanol mixture is mixed with 2,6-dihydroxy anthraquinone (0.3 g, 1.2×10^{-3} mol) dissolved in 25 mL of ethanol, and pH is set at 7 ± 0.2 with ethanolic KOH dilute solution. The mixture is warmed and stirred for 12 h at 65 °C evaporating its volume by half. After being cooled at room temperature, a red powder is filtered and washed with ethanol and acetone. Yield: 63%. Elem. Anal. for $C_{30}H_{36}O_4N_4Ni$ calculated (found)%: C, 62.41 (61.28); H_α, 6.63 (6.73); N, 9.70 (9.85). Decomposition: 220 °C. IR (KBr, cm^{-1}) ν max: 3448−3200 (O−H, N−H); 2875−3066 (C−H, CH_3); 1631−1558 (C=O, C=N); 1306, 1078 (C−O). MS (FAB) *m/e*: [M^+] 577; [M^+−238] 339; [M^+−339] 238. X-ray diffraction data for one 0.02 × 0.18 × 0.26 mm single crystal of this compound were obtained.

Synthesis of (racemic-5,7,7,12,14,14-hexamethyl-1,4,8,-11-tetraazacyclotetra-decane)Ni(II) 2,6-dihydroxyanthraquinonate diaquo-2H_2O (II). Ni(rac-5,7,7,12,14,14-hexamethyl-1,4,8,11-tetraazacyclotetradecane) perchlorate (1 g, 1.8×10^{-3} mol) dissolved in 10 mL of H_2O and 15 mL of ethanol is mixed with 2,6-dihydroxyanthraquinone (0.44 g, 1.852×10^{-3} mol) dissolved in 50 mL of ethanol. pH is set at 7 ± 0.2 with ethanolic KOH solution. The mixture is warmed to 65 °C with stirring for 12 h and reduced to half its volume. An orange solid is precipitated, filtered, and washed with acetylacetate and hexane. Yield: 45%. Elem. Anal. for $C_{44}H_{58}O_{14}N_4Ni$ calculated (found)%: C, 64.64 (64.98); H, 5.67 (5.45); N, 6.85 (6.72). Decomposition: 285 °C. IR (KBr) ν max: 3427 (O−H); 3249−3192 (N−H); 2972−2883 (C−H); 1637, 1545 (C=O); 1308, 1080 (C−O); 564 (Ni−O). MS (FAB) *m/e*: [M^++H] 919; [M^+−339] 580; [M^+−394] 525; [M^+−422] 497; [M^+−466] 453; [M^+−478] 441; [M^+−510] 409; [M^+−578] 341; [M^+−312] 307. X-rays diffraction data for a 0.66 × 0.16 × 0.08 mm single crystal of this compound were obtained.

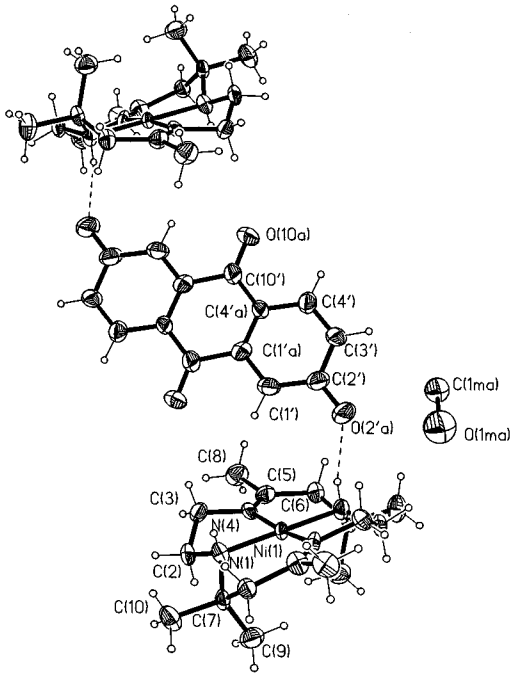

Figure 1. Details of the crystal structure showing the intermolecular interactions between macrocyclic Ni(II) cation **I** and 2,6-dihydroxyanthraquinone dianion.

Crystal Structure

Single-crystal X-ray structure determination was carried out using crystals from aqueous methanolic solutions.

Compound **I** crystallizes with a methanol molecule, in the monoclinic space group *C*2/*c*, and the asymmetric unit corresponds with half of the molecule. Compound **II** crystallizes with two coordinated and two crystallization water molecules, in the triclinic space group *P*1.

Data were collected on a Siemens P4 diffractometer. The structures were solved by direct methods and refined by full-matrix least-squares[15] with anisotropic temperature factors for the non-hydrogen atoms. The hydrogen atoms were included at idealized positions, all hydrogens with a fixed temperature factor $U = 0.08$ Å^2, except for hydrogen atoms binding to heteroatoms.

In the macrocyclic cation **I**, Ni(II) is located at the center of inversion, coordinated to four N atoms of the macrocyclic ligand, depicted in Figure 1. The coordinate geometry for Ni(II) is planar, with the two five-membered rings in gauche conformation and the two six-membered rings in twist conformation.

In complex **I**, the two N−hydrogen atoms are oriented to the same side with regard to the NiN_4 basal plane, whereas oriented to the opposite side of this basal plane,

(10) Simon, J.; André, J. J. *Molecular Semiconductors*; Springer-Verlag: Berlin, 1985.
(11) Ahmad, A.; Collins, R. A. *Thin Solid Films* **1992**, *217*, 75.
(12) Dodabalapur, A.; Katz, H. E.; Torsi, L.; Haddon, R. C. *Science* **1995**, *269*, 1560.
(13) Kido, J.; Kumura, M.; Nagai, K. *Science* **1995**, *267*, 1332.
(14) Douglas, B. H. *Inorg. Synth.* **1978**, *18*, 1−50.
(15) Sheldrick, G. M. *SHELEXT/PC User's Manual*, rel. 4.1; Siemens Analytica X-ray Instruments Inc.: Madison, Wisconsin, 1990.

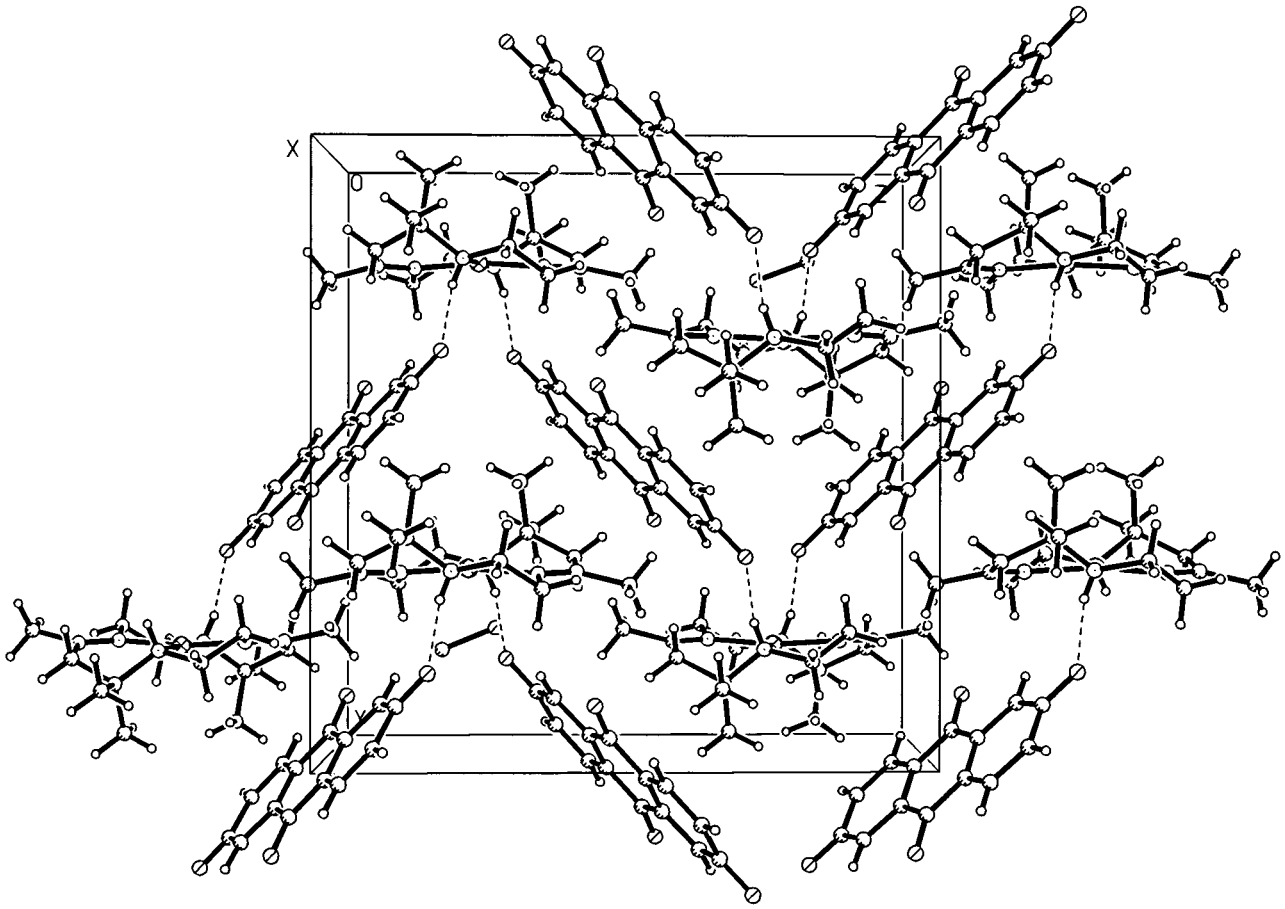

Figure 2. Crystal packing showing the hydrogen bond contacts determining the molecular accommodation.

there are four C-methyl groups bonding to Csp^3, and the other two C-methyl groups bonding to Csp^2 are over the same equatorial NiN_4 plane.

Hydrogen bonds between a 2,6-dihydroxy-anthraquinone dianion and NH group stabilize the crystal structure. Each 2,6-dihydroxy-antraquinone dianion is linked to two macrocyclic Ni(II) cations, as shown in Figure 1. Packing shows the 2,6-dihydroxy-anthraquinone dianion forming a zigzag layer that is sandwiched between two layers of Ni(II) complex, as shown in Figure 2.In the macrocyclic cation, **II** Ni(II) is located at the center of inversion, six-coordinate in a distorted octahedral environment, with the four N atoms of the macrocyclic tetradentate ligand in equatorial positions and the O atoms of two water molecules in axial position, as depicted in Figure 3. The macrocyclic tetradentate ligand is in a planar conformation, with the two five-membered rings in gauche conformation and the two six membered rings in chair conformation.

A view of the packing of the molecules in a unit cell is shown in Figure 4. In this projection, it is possible to see a Ni(II) complex layer between two parallel layers of the 2,6-dihydroxy-anthraquinone anion. Different intermolecular hydrogen bonds help to stabilize the crystal structure. $O_{2'}-H-O_{6'i}$, hydrogen bonds link the dihydroxy-anthraquinone anion into chains, whereas the O_2-H-O_{1w},O_2-H-O_{3w}, $O_{3w}-H-O_{1w}$, $O_{2w}-H-O_{3w}$, $O_{2w}-H-N_4$, and $O_{10}-H-O_{2w}$ hydrogen bonds cross-link these chains into a sheet and establish the interlayer connections. There are no direct bonds between the anion and the cation.

The Ni−N distances for **I** and **II** can be classified into two types: metal and amine N or metal and imine N atoms. These two types of bond distances are in agreement with previous results.

Thin Films: Experimental Section

Thin films were prepared to evaluate the conducting properties of complexes **I** and **II.** These studies are important for the potential application of these materials in the design of thin-film electronic devices, such as TFTs and gas sensors. Thin-film deposition was carried out by vacuum thermal evaporation. To prevent the powder products from spattering the surface of the substrate, the evaporation source was a molybdenum boat with two grids. The temperature of the evaporation boat was measured by means of a chromel−alumel thermocouple. The electrical current through the molybdenum boat was slowly increased up to 20 °C below the first significative change shown by the TGA thermogram to prevent thermal decomposition of the samples. For infrared and ellipsometric measurements, the used substrates were (100) oriented 200 $(\Omega\ cm)^{-1}$ C-Si slices. For optical transmission measurements, the substrates were naked 7059 Corning glass slices. Finally, for electrical measurements, the substrates were 7059 Corning glass coated with four metallic strips deposited by vacuum thermal evaporation.

Thin Films: Results and Discussion

X-ray spectra for all of the studied films present the typical pattern of amorphous material, although the

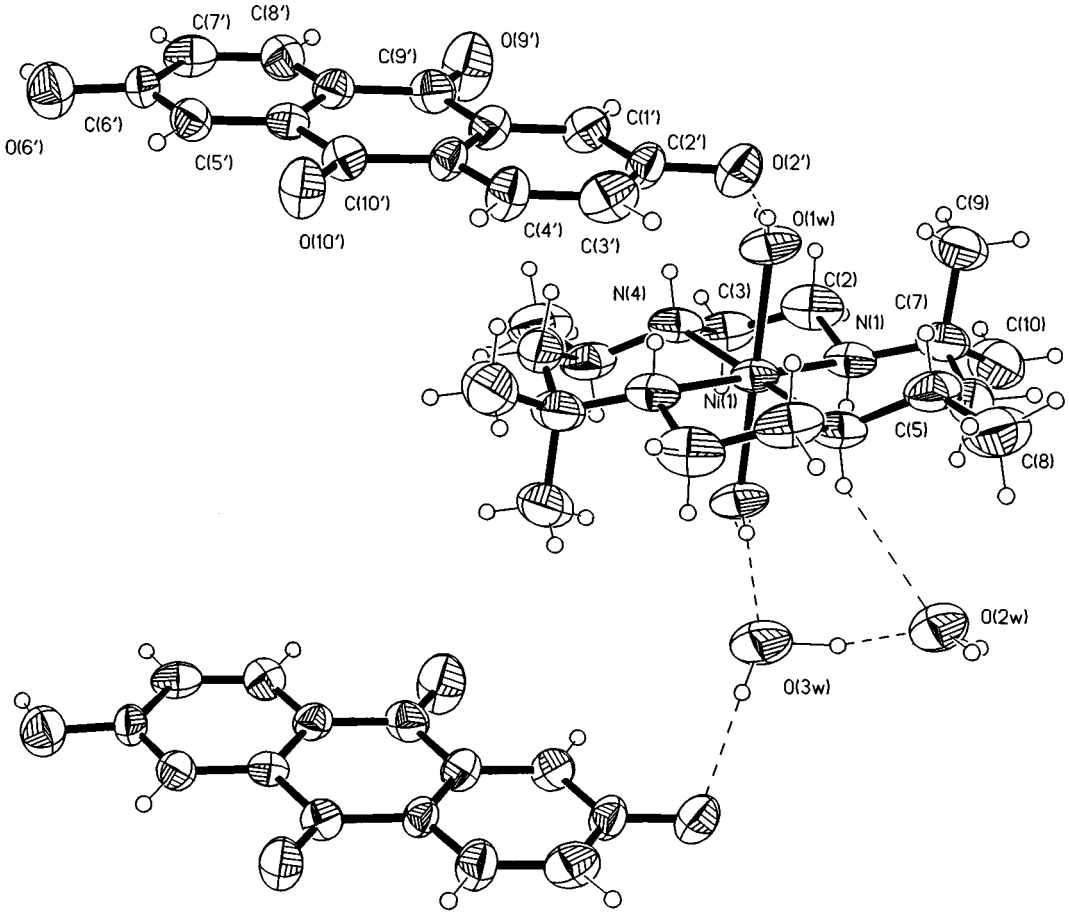

Figure 3. Details of the crystal structure showing the intermolecular interaction between macrocyclic Ni(II) cation **II**, 2,6-dihydroxyanthraquinone anion, and water molecules.

thickness of the deposited films (290−350 nm) is enough to observe peaks indicating crystallinity in polycrystalline films, even for small grain size. If it is considered that the substrate was kept at room temperature during evaporation, the macro-ions arriving on the surface of the substrate do not have enough energy, and hence surface mobility, to get a crystalline assembly.

Observed infrared peaks related to vibration modes of the intramolecular bonds indicate that the evaporation process does not have any effect on these bonds. The location of the IR peaks observed in the deposited films is slightly shifted in comparison to the corresponding peaks observed in the original powders. These differences are accounted for the fact that thin films deposited exhibit internal stress.[16] These results appear to indicate that the thermal evaporation and deposition processes are of molecular nature and the deposited films are formed by the same macro-ions as those of the original synthesized powder.

From ellipsometry measurements, the thickness and refractive index of the films are obtained, for a wavelength of 630 nm. By taking into account the refractive index values, an estimation of the optical reflectance (R) can be made.[17] Table 1 shows the results of the thickness (th), refractive index (n), and the estimated reflectance (in percentage) for the deposited films. The optical transmission results were analyzed by means of the Tauc model.[18] In this model, it is assumed that in electronic transitions from states of valence band to states of the conduction band there is no conservation of the electronic momentum. These transitions are called nondirect transitions. From the dependence of the calculated absorption coefficient as a function of the photon energy, the optical gap energy (E_{op}) values are determined.[19]

The current−voltage (I−V) characteristics were obtained at room temperature. The obtained values of the dark electrical conductivity (σ_d) are shown in Table 1. Given the ranges of applied voltages for each sample, the slope of the log I versus log V plots equals approximately 1 in all cases. This fact indicates that an ohmic behavior is observed. Figure 5 shows the dependence of the electrical conductivity of the film on the temperature during the measurement, at fixed voltages in the ohmic regime. The general behavior observed in these curves can be associated with semiconducting materials.

In amorphous semiconductors, it is known that states in the band tails are localized and they are separated from the extended states by a sharp energy known as a mobility edge. Thus, in the present case, the existence

(16) Alonso, J. C.; Ramirez, S. J.; Garcia, M.; Ortiz, A. *J. Vac. Sci. Technol.* **1995**, *A13*, 1.

(17) Bube, R. H. *Electronic Properties of Crystalline Solids*; Academic Press: New York, 1974.

(18) Ziman, J. M. *Models of Disorder*; Cambridge University Press: New York. 1979.

(19) Cody, G. D. In *Hydrogenated Amorphous Silicon*, Part B, Optical Properties: Semiconductors and Semimetals; Pankove, J. I., Ed.; Academic Press: Orlando, 1984; Vol. 21.

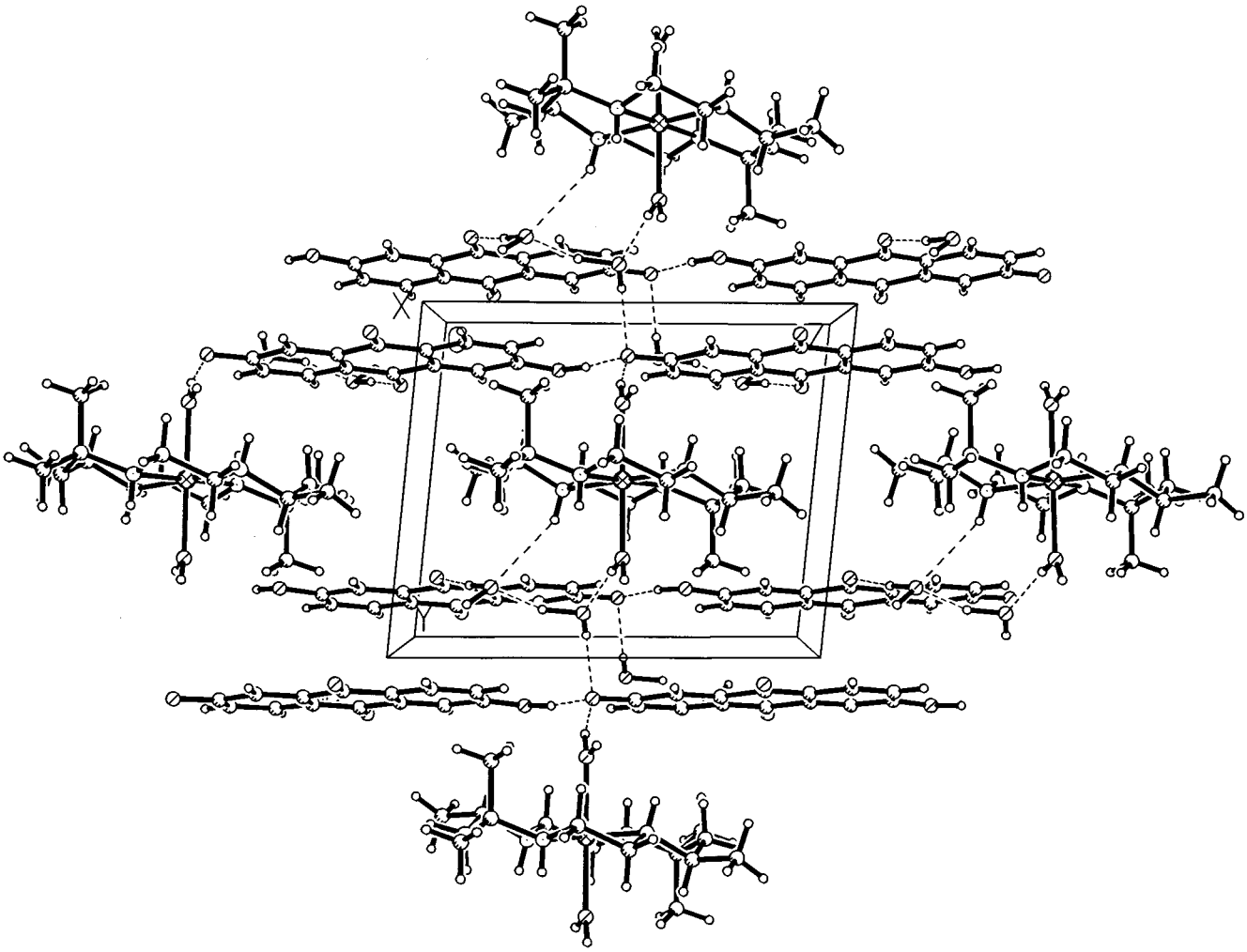

Figure 4. Crystal packing showing the different intermolecular hydrogen bonds helping to stabilize the crystal structure.

Table 1. Typical Measured and Calculated Parameters for the Thermal Evaporation Deposited Films of the Studied Compounds

	th (nm)	n	R (%)	E_{op} (eV)	σ_d $(\Omega\ cm)^{-1}$	E_{ac} (eV)
[Ni(*rac*-Me_6[14]aneN_4)] ($C_{14}H_6O_4$)	390	1.704	7	1.9	1.5×10^{-4}	1.8
[Ni(*meso*-Me_6[14]4,11dieneN_4)] ($C_{14}H_6O_4$)	387	2.481	18	2.0	3.3×10^{-6}	2.0

of a mobility edge means that the electrical conduction is associated with excited electrons from localized states through the mobility edge, so that the electrical conductivity behaves as $\sigma = \sigma_m \exp(-\Delta Em/kT)$, where ΔEm is the activation energy to delocalize the charge carriers.

On the other hand, for most organic materials, the phenomenological equation for the temperature dependence of the electrical conductivity is

$$\sigma = \sigma_o \exp(-\Delta E_{ac}/2kT) \qquad (1)$$

where ΔE_{ac} is an activation energy of unspecified nature. If the energy band model is considered, this activation energy is associated with the difference between the edge of the valence band and the edge of the conduction band. The linearization of the plots in Figure 5, indicated by the straight lines, gives the value of the activation energy at high temperatures. The ΔE_{ac} determined values are shown in Table 1.

Taking into account the optical and electrical properties of the deposited films, it appears to be possible to apply these materials to the preparation of electronic devices.

Theoretical Studies

To investigate possible mechanisms involved in the semiconducting behavior of compounds **I** and **II**, we decided to carry out molecular structure calculations on our two compounds. These calculations were at ab initio level, using the restricted Hartree−Fock (RHF) method, which has been successfully applied in molecules containing transition metals.[20] To save computational effort, we applied the effective core potential (ECP) approximation to substitute the core electrons of Ni. For the other atoms, all of their electrons were considered explicitly. In our calculations, we used two different conformations for each compound. First, we considered the crystalline structure and, as a second conformation, those obtained from a Molecular Dynamics run at 400 K. This procedure gave us the opportunity to sample a

(20) Cogordan, J. A.; Gómez-Lara, J.; Cabrera, A.; Rosas, N. *J. Mol. Struct. (THEOCHEM)* **1997**, *392*, 223−230.

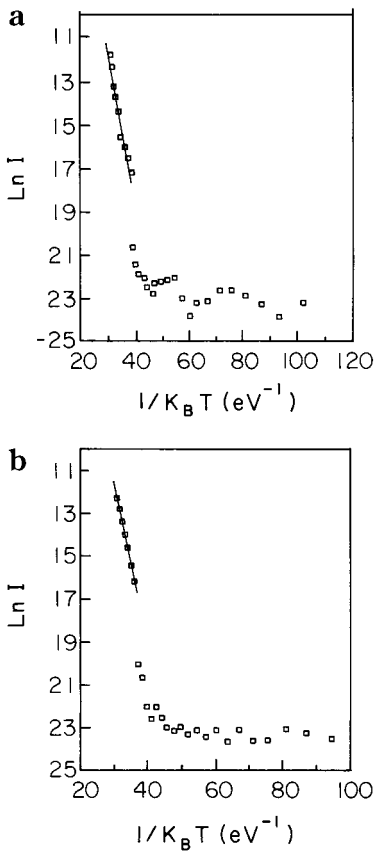

Figure 5. Electrical current as a function of the temperature during the measurement of (a) [Ni(*meso*-Me_6[14]4,11dieneN$_4$)]-($C_{14}H_6O_4$) (**I**) and (b) [Ni(*rac*-Me_6[14]aneN$_4$)]($C_{14}H_6O_4$) (**II**).

set of minima energy conformations. We selected only those conformations with the lowest energy for each compound. In these steps, we used the esff force field implemented in the *Discover* program.[21]

Our molecular structure calculations were carried out with the suite of programs in *Gaussian 94*.[22] The ECP used for Ni considers some of the most important relativistic effects.[23] In all of our SCF calculations, we used minimal basis sets. No formal charge was considered on compounds **I** and **II**, since in our calculations we included explicitly the complexes and their respective counterions.

With the computed density matrix and molecular orbitals (MO) a local density of states (LDOS) was calculated. This LDOS has successfully been applied to study electron conformation of Si-based semiconductors.[24]

Theoretical Results

In Table 2, the computed RHF energies for **I** and **II** are reported. It may be observed that the value $\Delta E_{(L-H)}$ is larger for the optimized conformation. In the last row of this table, we report the optimized conformation when the water molecules have been removed. We suppose that this must be the case, as during the vacuum thermal evaporation process, these water molecules should be removed. As in the previous case, we obtained a number of conformations and only the one with the smallest energy is considered for calculations. It is important to mention that in this last conformation, the two dihydroxyanthraquinones are on opposite sides of the Ni.

Table 2. Computed Energies for I and II[a]

compound	total energy (au)	HOMO (au)	LUMO (au)	ΔE_{L-H} (eV)
I C	−1821.78	−0.0056	−0.06	1.50
I O	−1822.24	−0.06	0.03	0.92
II C	−2797.04	0.002	0.02	0.41
II O	−2798.16	−0.09	0.03	1.52
II ONW	−2648.33	−0.09	0.009	2.09

[a] C stands for crystalline coordinates. O stands for minimal energy coordinates. ONW stands for compound **II** without coordinated water molecules.

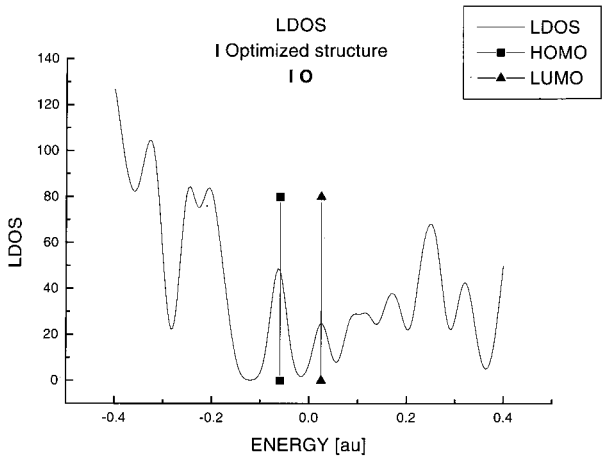

Figure 6. LDOS for the optimized structure of compound **I**. HOMO and LUMO are marked ■ and ▲, respectively. Calculations were done with RHF. Energy units are in atomic units.

In Figures 6−8, the calculated LDOS for conformations reported in the second, fourth, and fifth rows of Table 2 are depicted. It may be observed that for the cases where no water molecules are included, there is a non-zero LDOS close to the HOMO and LUMO. For **I** and **II**, their HOMO are formed from atomic orbitals (AO) of the oxygen atoms located in the dihydroxyanthraquinones. Some molecular orbitals below the HOMO are constituted by AO from the N and C atoms of the Ni entity and some O and C from the dihydroxyanthraquinone unit. This may be indicative of a possible channel for a charge-transfer mechanism between these two molecular units. In all of the computed cases, the major contribution to the LUMO formation comes from the d AOs of the Ni atom.

Discussion of Theoretical Results

All of our experimental evidence shows that the studied thin films of this report, obtained by chemical vapor deposition, are amorphous. In this way, the

(21) *Discover V 95.0*, molecular simulation program comercially available from Molecular Simulations Inc.: San Diego, CA.

(22) Frisch, M. J.; Trucks, G. W.; Schlegel, H. B.; Gill, P. M. W.; Johnson, B. G.; Robb, M. A.; Cheeseman, J. R.; Keith, T.; Petersson, G. A.; Montgomery, J. A.; Raghavachari, K.; Al-Laham, M. A.; Zakrzewski, V. G.; Ortiz, J. V.; Foresman, J. B.; Cioslowski, J.; Stefanov, B. B.; Nanayakkara, A.; Challacombe, M.; Peng, C. Y.; Ayala, P. Y.; Chen, W.; Wong, M. W.; Andres, J. L.; Replogle, E. S.; Gomperts, R.; Martin, R. L.; Fox, D. J.; Binkley, J. S.; Defrees, D. J.; Baker, J.; Stewart, J. P.; Head-Gordon, M.; Gonzalez, C.; Pople, J. A. *Gaussian 94*, rev. E.2; Gaussian, Inc.: Pittsburgh, PA, 1995.

(23) Hay, P. J.; Wadt, W. R. *J. Chem. Phys.* **1985**, *82*, 270; 284; 295.

(24) Cogordan, J. A.; Sansores. L. E.; Valladares. A. A. *J. Non-Cryst. Solids* **1995**, *181*, 135−145.

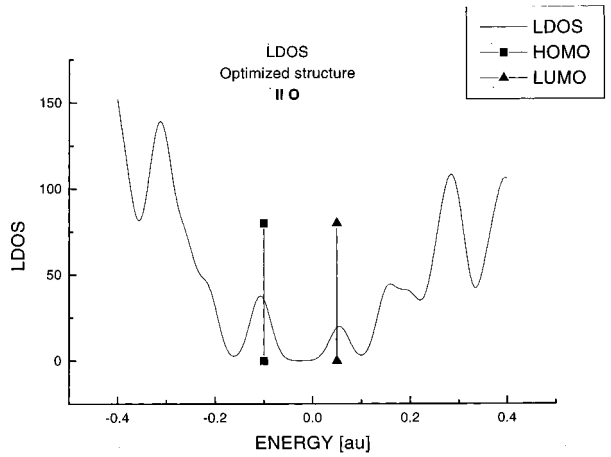

Figure 7. LDOS for the optimized structure of compound **II**. In this case, the coordinated water molecules are considered explicitly for the calculations. HOMO and LUMO are marked ■ and ▲, respectively. Calculations were done with RHF. Energy units are in atomic units.

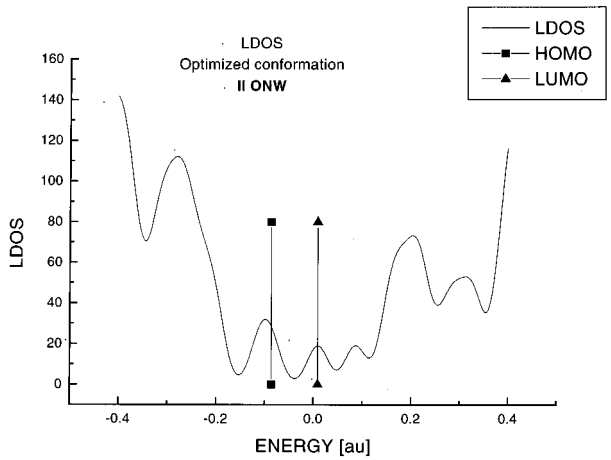

Figure 8. LDOS for the optimized structure of compound **II**. In this calculation, the coordinated water molecules have been removed. HOMO and LUMO are marked ■ and ▲, respectively.Calculations were done with RHF. Energy units are in atomic units.

conformation of the NiN_4 entity and the dihydroxyanthraquinone may be different than the one present in the crystalline form, retaining the 1:1 and 1:2 stoichiometric relations, for **I** and **II**, respectively. Furthermore, according to Tauc,[19] the electronic behavior of an amorphous solid is strongly related to the molecule itself and to its first neighbors. With these ideas, we may conclude that our calculations show the same trend as our experimental results, which may be used as a model for an explanation. It is convenient to mention that all of our calculations, MD, MM, and HF, were carried out in a vacuum and with an isolated molecule. This should then only be considered as a limited model for the phenomena in an amorphous state.

Analyzing the energy gaps in Table 2, we observe that they are close to the reported experimental values of the deposited thin films of molecules **I** and **II**. The discrepancies may be due to the fact that minimum energy criterion might not be the most appropriate for the packing of an amorphous solid.

The reported $\Delta E_{(L-H)}$ of 2.09 eV in the last row of Table 2 is in excellent agreement with the 2.0 eV obtained experimentally. The small energy difference for the crystalline structure of **II**, the third row in Table 2, may be due to a shortening of the bond lengths and angles in the crystalline conformation.

From the LDOS plots shown in Figures 6−8, it is possible to conclude that there is a density of states close to the energy gap. These states are formed mainly with p atomic orbitals from the carbon and oxygen, located in the dihydroxy-anthraquinone molecular entities. This last statement is valid for the optimized conformations of compounds **I** and **II**.

Conclusions

Crystal packings show large tetraaza Ni coordinated dications and anthraflavic dianions regularly interpersed for the unsaturated system, whereas hydrogen-bonded tapes of anthraflavic ions forming sheets in the crystal are present in the saturated derivative.

Measurements of conductivity on amorphous thin films obtained by chemical vapor deposition indicate a low-dimensional behavior with a conductivity on the order of that shown by organic semiconductors.

IR spectroscopy results for the synthesized powders and their corresponding deposited thin films indicate that the atomic intramolecular bonds remain the same, and X-ray diffraction spectra for the deposited films show an amorphous nature, suggesting that thermal evaporation can be described as a molecular process and that the substrate temperature is not high enough to give a suitable surface mobility to produce crystalline films. Sample change with temperature was determined by TGA measurements.

By taking into account the Tauc model of optical absorption for amorphous semiconductors, optical absorption edge values were determined from the optical transmission measurements. These values are similar to those determined for the electrical conductivity activation energy by means of the temperature dependence of the electrical conductivity. These results indicate that, in these materials, the dominant levels are the conduction and the valence bands showing a semiconductor behavior. However, more work is necessary to obtain thin films with crystalline nature, with the possible increase of electrical conductivity.

To obtain the molecular orbital energy levels and local density of electronic states, ab initio calculations were carried out using the restricted Hartree−Fock method.

Our LDOS results clearly show the influence of the dihydroxy anthraquinone on the electronic structure in both compounds. Its main activity is to bring electronic states at the HOMO energy level. This provides a richer electronic structure which reduces the gap of the NiN_4 entity. Our calculations do not attempt to fully explain the electronic conformation of an amorphous solid; however, they give a clear picture of the possible mechanism in the semiconducting behavior of the two compounds in this report.

Acknowledgment. The authors thank L. Baños, C. Vázquez, and K. Ebert for technical assistance, and Dr. Juan C. Alonso for helpful discussions. We thank the partial financial support by CONACyT, México, Grants 1642E, F192, F592, 25793-E. J.A.C. is grateful to Professor Samuel Tricky for interesting discussions in

an early stage of this project, and to DGSCA, UNAM, for the generous allocation of CPU time in the Cray YMP and in the Origin 2000 supercomputers.

Supporting Information Available: Atomic coordinates and equivalent isotropic displacement coefficients, bond lengths and angles, anisotropic displacement coefficients, and H atom coordinates and isotropics for **I**. This material is available free of charge via the Internet at http://pubs.acs.org.

CM990138K